Protein Dynamics in the Region of the Sixth Ligand Methionine Revealed by Studies of Imidazole Binding To *Rhodobacter capsulatus* Cytochrome c_2 Hinge Mutants[†,‡]

C. Dumortier,[§] J. Fitch,[§] F. Van Petegem,[∥] W. Vermeulen,[∥] T. E. Meyer,[§] J. J. Van Beeumen,[∥] and M. A. Cusanovich*,[§]

Department of Biochemistry and Molecular Biophysics, University of Arizona, Tucson, Arizona 85721, and the Department of Protein Biochemistry and Protein Engineering, University of Ghent, Ledeganckstraat 35, 9000 Ghent, Belgium

Received December 12, 2003; Revised Manuscript Received April 22, 2004

ABSTRACT: All class I c-type cytochromes studied to date undergo a dynamic process in the oxidized state, which results in the transient breaking of the iron-methionine-sulfur bond and sufficient movement to allow the binding of exogenous ligands (imidazole in this work). In the case of *Rhodobacter capsulatus* cytochrome c_2, the sixth heme ligand Met96 and up to 14 flanking residues (positions 88−100, termed the hinge region), located between two relatively rigid helical regions, may be involved in structural changes leading to a transient high-spin species able to bind ligands. We have examined 14 mutations at 9 positions in the hinge region of *Rhodobacter capsulatus* cytochrome c_2 and have determined the structure of the G95E mutant. Mutations near the N- and C-terminus of the hinge region do not affect the kinetics of movement but allow us to further define that portion of the hinge that moves away from the heme to the 93−100 region in the amino acid sequence. Mutations at positions 93 and 95 can alter the rate constant for hinge movement (up to 20-fold), presumably as a result of altering the structure of the native cytochrome to favor a more open conformation. The structure of one of these mutants, G95E, suggests that interactions within the hinge region are stabilized while interaction between the hinge and the heme are destabilized. In contrast, mutations at positions 98 and 99 alter imidazole binding kinetics but not the hinge movement. Thus, it appears that these mutations affect the structure of the cytochrome after the hinge region has moved away from the heme, resulting in increased solvent access to the bound imidazole or alter interactions between the protein and the bound imidazole.

Class I cytochromes c are primarily low-spin due to the presence of the strong-field heme ligands, histidine and methionine, and the ferrous form does not normally bind exogenous ligands. However, it is well established that the ferric form of mitochondrial cytochrome c and the bacterial cytochromes c_2 undergo a dynamic rearrangement that results in breakage of the iron−methionine bond and in the formation of a low concentration of high-spin species that permits weak binding of exogenous ligands (*1*−*3*). In all cases, it has been found that imidazole binding is a two-step process involving a rate-limiting protein rearrangement followed by second-order ligand binding (*2*−*4*), as illustrated in equation 1 where cyt[1] is the native closed, unreactive form and cyt* is the open form that binds imidazole. The rate constant for rearrangement is k_{12}, and the apparent binding constant is $K_{app} = K_1K_2/(1+ K_1)$, where $K_1 = k_{12}/k_{21}$ (equilibrium between the open and closed forms), and $K_2 = k_{23}/k_{32}$ (ligand binding).

$$\text{cyt} \underset{k_{21}}{\overset{k_{12}}{\rightleftharpoons}} \text{cyt*} + \text{imidazole} \underset{k_{32}}{\overset{k_{23}}{\rightleftharpoons}} \text{cyt*-imidazole} \quad (1)$$

The protein rearrangement coupled to ligand binding occurs in a region (termed the hinge) between two sections of secondary structure (*4*), helices 84−91 and 107−119, in *Rhodobacter sphaeroides* cytochrome c_2 (helices 80−87 and 104−114 in *Rhodobacter capsulatus* cytochrome c_2). In Figure 1A, the α-carbons for the hinge region (positions 92−106) of the native form and of the imidazole complex (*5*) of *Rb. sphaeroides* cytochrome c_2 are overlaid (the structure of the *Rb. capsulatus* cytochrome c_2−imidazole complex has not been determined). Also shown in Figure 1A are the heme and bound waters. Note that the overlay suggests that the hinge region may be constrained to positions 97−105 (93−100 in the *Rb. capsulatus* cytochrome c_2 amino acid sequence) since the backbone in the 92−96 and 106 regions are the same in free and complexed structures (Figure 1A and 1B). Figure 1B shows the overlay of *Rb. sphaeroides*

[†] This work was supported in part by a grant from the National Institutes of Health, GM 21277 to M.A.C. and from the fund for Scientific Research, Flanders, 36042298 to JVB.

[‡] The PDB accession code for the structure of *Rb. capsulatus* cytochrome c_2 mutant G95E is 1ryd.

* To whom correspondence should be addressed. Tel.: 520-621-7533. Fax: 520-621-6603. Email: cusanovi@u.arizona.edu.

[§] University of Arizona.

[∥] University of Ghent.

[1] Abbreviations: G95E, glutamic acid substituted for glycine 95 in *Rb. capsulatus* cytochrome c_2 (other mutations follow the same format); 10V11/K93G, a double mutant containing an insertion of a valine between positions 10 and 11 in the K93G background; VK93G, shorthand notation for the 10V11/K93G double mutant; cyt, native folded form of oxidized cytochrome c that does not bind exogenous ligands; cyt*, high-spin form of oxidized cytochrome c capable of binding ligands; PDB, protein data bank.

10.1021/bi0362370 CCC: $27.50 © 2004 American Chemical Society
Published on Web 05/28/2004

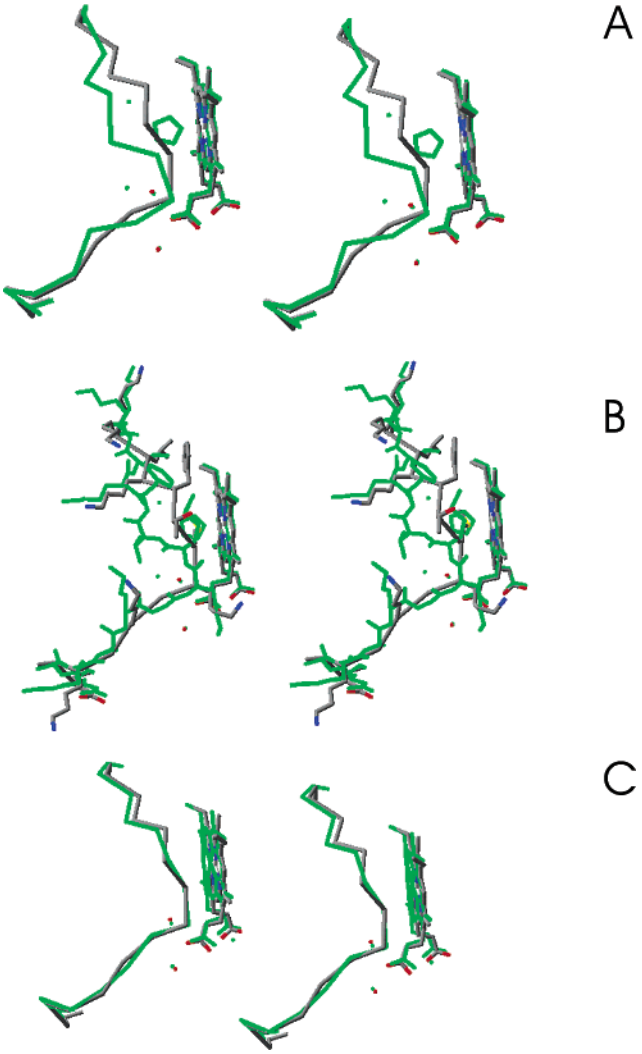

FIGURE 1: (A) Superposition of the hinge α-carbons, hemes, and bound waters of the native and the imidazole complex of *Rb. sphaeroides* cytochrome c_2 (*5*). The imidazole complex is in green, and the uncomplexed cytochrome c_2 is in CPK colors (carbon gray). (B) Superposition of the hinge backbone atoms, side chains, hemes, and bound waters of the native and the imidazole complex of *Rb. sphaeroides* cytochrome c_2. Colors as in A. (C) Superposition of the hinge α-carbons, hemes, and bound waters of *Rb. sphaeroides* (green) and *Rb. capsulatus* (CPK) cytochrome c_2.

cytochrome c_2 and its imidazole complex in the hinge region and includes backbone and side chain atoms. This illustrates the large movement in some of the side chains, including those of M100 and F102. Figure 1C presents an overlay of the hinge region α-carbons, bound waters, and hemes of *Rb. sphaeroides* and *Rb. capsulatus* cytochrome c_2. As can be seen, there is considerable structural homology between the cytochromes c_2 from the two species (9 out of the 15 hinge amino acids are the same). This is consistent with the fact that imidazole binding (equilibrium and kinetics) are identical for the two species (3). Thus, in the context of eq 1, we have structural information relative to cyt and cyt*−imidazole species, but not for cyt*, the open conformation without ligand. Cyt*−imidazole is likely to be a more closed, less dynamic, structure than cyt* because of the stabilizing interactions between the surrounding protein and the bound imidazole.

There has been speculation that rearrangement of the hinge in the absence of imidazole may have a role in electron transfer since this rearrangement occurs in a structural region involved in binding to reaction partner proteins (*6*). Because the rearrangement is specific to the oxidized form of the protein, it may provide a mechanism to signal the change in oxidation state during physiological electron transfer, altering the binding constant and product dissociation. However, no data are currently available that directly address this view. The analogous hinge region in horse cytochrome c includes residues 77−85 (*7*). The apparent binding constant for imidazole (K_{app}) is much larger with *Rb. capsulatus* (1440 M^{-1}) and *Rb. sphaeroides* (1420 M^{-1}) cytochrome c_2 than it is for horse cytochrome c (30 M^{-1}), but the kinetics of rearrangement (k_{12}) are comparable for all three (27−42 s^{-1}) (*3*). Studies of imidazole binding by mutants of *Rb. capsulatus* cytochrome c_2 showed that most are similar to wild-type protein (i.e., within a factor of 2), but with some exceptions that bind imidazole more strongly and rearrange more rapidly (*4*, *8*). The exceptions (G95E and G95P), which are located in the hinge region, appear to alter the kinetics of the rearrangement (k_{12}, k_{21}). It is important to note that mutants with substantially altered hinge kinetics and an altered equilibrium between the open and closed forms (eq 1) may provide a means to test proposals in regard to the physiological role of the hinge.

In the past, we had insufficient data to specify all four rate constants for imidazole binding. More recently, however, we found that mutant G95P has much greater high-spin character than wild-type protein in equilibrium with the normal low-spin species (i.e., K_1 is 55-fold larger than for wild-type cytochrome) (*8*). This additional information has permitted resolution of all four rate constants for the mutant, and by extrapolation, for wild-type protein, by assuming that the rate constant for imidazole binding, k_{23}, is the same for both the wild-type cytochrome and the G95P mutant (i.e., 1.4×10^5 $M^{-1}s^{-1}$). We have now studied imidazole binding for additional hinge mutants of *Rb. capsulatus* cytochrome c_2 to determine the role of individual sequence positions in hinge dynamics and to further define the hinge region.

MATERIALS AND METHODS

Rb. capsulatus cytochrome c_2 and mutants were prepared as previously described (*9*). Imidazole was purchased from Sigma Chemical Co. The equilibrium binding of imidazole was studied by measuring the peak-to-trough difference in amplitude due to the increase in absorbance at 405 nm and the decrease at 417 nm. All experiments were carried out in 100 mM Tris-cacodylate buffer, pH 7, supplemented with sodium chloride to maintain constant ionic strength. All solutions contained 100 μM potassium ferricyanide to maintain cytochrome c_2 in the oxidized state. Equilibrium titrations and kinetic experiments were carried out at 500 mM ionic strength to allow the use of a wide range of concentrations of imidazole (which has a pK_a of 7) and that contributes substantially to the ionic strength. Equilibrium and kinetic data were analyzed relative to eq 1 as described previously (*3*). All equilibrium constants and second-order rate constants are given in terms of the concentration of unprotonated imidazole.

We were unable to obtain the K93G single mutant, presumably because it is too unstable. Thus, we constructed the double mutant 10V11/K93G, which includes an insertion

of valine between residues 10 and 11 that we have found is a strongly stabilizing mutation, which permits folding. Our shorthand notation for this mutant is VK93G.

Circular dichroism spectra were measured with an Aviv-modified Cary 60 spectropolarimeter. Denaturation was studied by changes in ellipticity at 220 nm as a function of guanidine in 20 mM Tris-Cl, pH 7.5, 40 mM NaCl. Two parameters were obtained from the data, the midpoint concentration (C_m) and the slope (m) of the log plots. The midpoints are highly reproducible, but in our experience, the variation in slope from one experiment to the next was equal to the differences among most mutants. Therefore, we report only the C_m.

The reduced form of the G95E mutant was crystallized under conditions very similar to those described for the wild-type protein (*10*). Crystals used for structure determination grew in hanging drops against a well solution containing 3.5−3.6 M $(NH_4)_2SO_4$, 50 mM Tris-HCl pH7.5, and 200 mM NaCl, using 2 + 2 μL drops and a 4.5 mg mL^{-1} protein stock solution. Like the wild-type protein, the G95E mutant crystallizes in the *R*32 space group with cell parameters $a = b = 100.23$ Å, $c = 162.15$ Å, containing two molecules in the asymmetric unit. The initial model based on wild-type cytochrome c_2 was refined against data to 2.3 Å of 88% completeness and I/sigma 13.27 (3.2, outer resolution shell) and R_{merge} 8.7% (33%) to final *R*- and free *R*-factor of 19.8 and 24.2%.

Structures were modeled with the Deep View/Swiss-Pdb Viewer software (http://www.expasy.org/spdbv/).

RESULTS

Equilibrium Imidazole Binding. From our previous work comparing wild type *Rb. capsulatus* cytochrome c_2 with mutations distributed throughout the structure, we found that both G93E and G95P had increased affinity for imidazole as compared to wild type and most other mutants (*4*, *8*). Thus, it appeared likely that other mutations in the hinge region would significantly alter imidazole binding and kinetics. We have now examined 13 additional mutants in the hinge region to establish their importance for imidazole binding and protein dynamics. Figure 2A shows the difference absorbance spectra at various concentrations of imidazole for binding to mutant K90E. Figure 2B is the double reciprocal plot of the data from which the apparent binding constant, K_{app}, was determined. Values of K_{app} are given in Table 1 for all the mutants studied. The difference spectra are generally similar to that of the wild-type protein. However, in some cases, the titrations indicate the presence of high-spin heme with a trough at 395 nm (G95E, G95P, see Figure 3A). In addition, in a number of cases, absorbance in the 600−650 nm region, indicative of high-spin heme, is found (G95E, G95P, G95K, and K93P, see Figure 3B).

The apparent affinities for imidazole were similar to wild-type for many hinge mutants but were much larger as compared to wild-type for mutations at positions 93 and 95. Mutants K93P, VK93G, G95P, G95E, and G95K showed significant increases in affinity for imidazole relative to wild type (7−30-fold), but K93E was like wild type. Mutant M96N, in which the sixth heme ligand was replaced by the weak field ligand asparagine (*11*), bound imidazole almost 400 times more strongly than wild type.

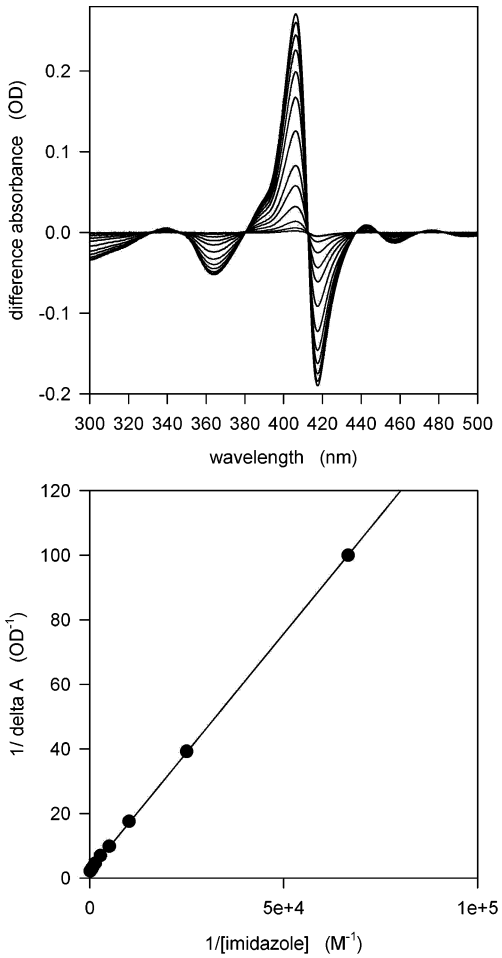

FIGURE 2: (A) Titration of *Rb. capsulatus* cytochrome c_2 mutant K90E (10 μM) with imidazole (8.3 μM−1.08 mM) at pH 7 and 25 °C. (B) The inverse of the total peak to trough absorbance changes at 408 and 418 nm was plotted against the inverse of the imidazole concentration to obtain the binding constant K_{app}.

Stopped-Flow Kinetics. As found for wild-type cytochrome c_2, all of the mutants studied had rate constants that became independent of imidazole concentration at high ligand concentrations (Figure 4). In the context of eq 1, the plots of the observed rate constants as a function of ligand concentration reflect a change in the rate-limiting step and can be analyzed, as previously reported, to obtain values for the individual rate constants k_{12} and k_{32}, and using the measured apparent affinity for ligand (K_{app}), a value for k_{23}/k_{21}. The measured rate constants and K_{app} are summarized in Table 1. In previous work, we determined the value of K_1 for the G95P mutant because sufficient high-spin cytochrome (cyt* in eq 1) was present to permit a direct measurement. Thus, k_{21}, k_{23}, and K_2 could be computed for imidazole binding. Further, assuming that k_{23} would be the same for G95P and wild-type cytochrome c_2, we were able to estimate all kinetic parameters for wild-type cytochrome c_2. We argued that since the mutation at position 95 is in the hinge, which swings out in the transiently open form (cyt*, eq 1), it would presumably affect rearrangement but would have less influence on the heme electronic structure and direct ligand binding (k_{23}) per se. On further reflection, and observing the variation in k_{32} (Table 1), we now believe a better assumption is that the ratio k_{23}/k_{32} (K_2) is less affected than is k_{23} alone. In Table 1, we have calculated k_{23}, k_{21} and

Table 1: Imidazole Binding Properties of *Rb. capsulatus* Cytochrome c_2 and Selected Mutants

cyto	$K_{app} \times 10^{-3}$ (M^{-1})	k_{12} s^{-1}	$k_{32} \times 10^{2}$ (s^{-1})	k_{23}/k_{21} (M^{-1})	$k_{23} \times 10^{-4}$ (M^{-1} s^{-1})	$k_{21} \times 10^{-4}$ (s^{-1})	$K_1 \times 10^3$
WT	1.44	27.4	6.3	3.3	6.3	1.9	1.4
K90E	1.56	30.0	5.3	2.8	5.3	1.9	1.6
K91E	1.18	28.4	6.9	2.9	6.9	2.4	1.8
K93E	1.33	25.7	5.5	2.8	5.5	2.0	1.3
A101P	1.79	51.0	3.0	1.0	3.0	3.0	1.7
A101G	2.00	36.5	6.5	3.5	6.5	1.8	2.0
K102E	1.99	48.1	3.6	1.8	3.6	2.0	2.0
M96N	568				NA	NA	NA
K93P	42.3	651	10.6	7.0	11	1.6	43.0
VK93G	11.0	86.3	16	20	16	0.8	11.0
G95E	44.4	280	9.5	15	9.5	0.6	47.0
G95K	22.0	55.1	16	64	16	0.2	22.0
G95P	30.0	53.8	16.8	70	14	0.2	30.0
F98S	6.10	40.0	80	120	80	0.7	6.0
K99E	2.30	26.1	24	21	24	1.1	2.3

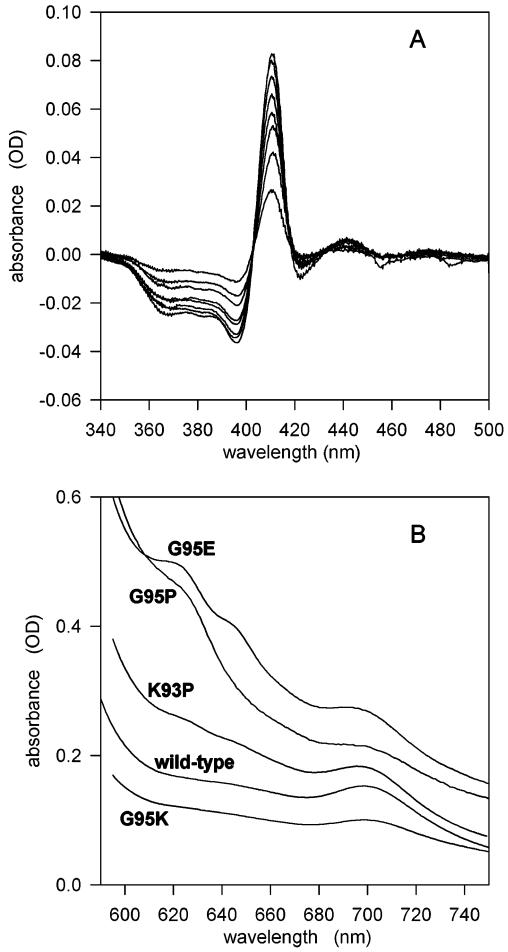

FIGURE 3: (A)Titration of *Rb. capsulatus* cytochrome c_2 mutant G95P (10 μM) with imidazole (3.0 μM−0.7 mM) at pH 7 and 25 °C. The data were analyzed as in Figure 2 (not shown). (B) Near-IR absorbance of wild-type, K93P, G95E, G95P, and G95K. Protein concentrations were typically 500 μM, and the spectra taken in a universal buffer (2 mM PIPES, MES, MOPS, HEPES, BICINE, and citrate) supplemented with 100 mM NaCl, pH 7. The spectra shown were offset to illustrate the shape, not the absolute absorbance.

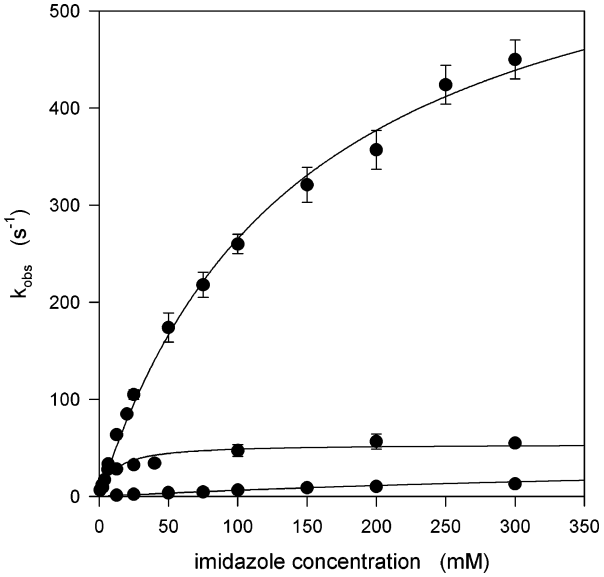

FIGURE 4: Concentration dependence of the observed rate constant, k_{obs}, for the binding of imidazole to *Rb. capsulatus* cytochrome c_2 mutants K93P (upper curve), G95P (middle curve), and K102E (lower curve). The solid line is a fit to the data using the explicit solution to eq 1 (*3*).

$K_1(k_{12}/k_{21})$ using a value of 1×10^6 M^{-1} s^{-1} for K_2 as determined experimentally for imidazole binding to the G95P mutant.

The mutants (and wild-type) summarized in Table 1 can be divided into four groups. In the first group are those which have basically the same kinetic parameters for imidazole binding as wild-type protein. M96N as the sole representative of group 2 is unique in binding imidazole via a simple equilibrium with an overall binding constant (5.7×10^5 M^{-1}), which approaches the value of K_2 measured for the G95P mutant, presumably reflecting the fact that M96N is predominantly high-spin. A third group of mutants, at positions 93 and 95, has significantly increased apparent overall affinities for imidazole and significantly larger values of k_{23}/k_{21}, as compared to wild-type cytochrome c_2. Finally, there are two mutants (F98S and K99E) in group 4, which have increased values of k_{32} and k_{23}/k_{21}. Note that the data analysis (K_1) predicts that five of the mutants in the elevated affinity group will have values of K_1 consistent with greater than 1% of the mutant being in a high-spin form, which should be detectable. In fact, either the titrations (Figure 3A) or spectroscopy in the 600−650 nm region (Figure 3B), or both, provide evidence for the presence of the high-spin form with mutants K93P, G95E, G95K, and G95P. VK93G is predicted to have about 1% high-spin species, but this was not detectable spectrophotometrically. This may be a consequence of the value being near the limit of spectroscopic detection.

Table 2: Physical−Chemical Properties of *Rb. capsulatus* Cytochrome c_2 and Selected Mutants

cyto	C_M (M)	pK_{695}	cyto	C_M (M)	pK_{695}
wild-type	1.61	9.6/11.1(72%)	K93P	1.18	7.7
K90E	1.65	9.3/11.3(43%)	VK93G	1.78	8.4
K91E	1.76	9.4/11.3(39%)	G95E	1.13	7.6
K93E	1.69	10.3/12.1(41%)	G95K	1.39	7.4
A101P	1.66	9.8/12.2(30%)	G95P	1.20	7.2
A101G	1.60	8.8/10.5(49%)			
K102E	1.54	9.9/12.3(46%)	F98S	1.36	9.6/11.8(34%)
			K99E	1.36	7.1
M96N	2.46	NA			

Physical−Chemical Properties. Table 2 summarizes the guanidine concentration for half-denaturation from circular dichroism titrations in the far UV, and the pK_a for the loss of the 695 nm absorption band at alkaline pH for the mutants and wild-type cytochrome c_2. For all of the group 1 mutants and most of the group 3 mutants, the *m* values for the guanidine titrations were similar to that for wild-type cytochrome c_2. Note that the 695 nm titrations for wild-type and for the mutants, which behave like wild-type protein with respect to imidazole binding, are complex with two pK_a values derived from the titration (the percentage contribution of the lower pK_a is given in parentheses). However, for those mutants with altered kinetic properties, where the pK_a is less than 9, they titrate as a single component. The mutants with pK_a values above 9 are subject to strongly alkaline conditions during the titrations, which presumably facilitates conversion to a denatured form which has a pK_a value near pH 11 and *n*-values greater than one.

G95E Structure. The G95E mutant crystallizes in the same space group as the wild-type cytochrome and has a backbone structure almost identical to that of the wild-type cytochrome. The rms deviations for comparison of the alpha carbons of wild-type and G95E are 0.20, and there is an rms of 0.23 for all backbone atoms. Figure 5A shows the hinge and adjacent regions of the wild-type protein including apparent hydrogen bonds (Deep View/Swiss-PdbViewer). There are 15 hydrogen bonds involving the hinge (88−102), residues 75−78, residues 54−57, the heme and bound waters (left, center, and right in the view shown) and a coordination bond between the heme iron and the methionine sulfur in the wild-type cytochrome c_2. The same bonds, with the same bond lengths (within 0.2 Å) are found in the G95E mutant crystal structure (Figure 5B). Five additional, relatively long hydrogen bonds, are found in the G95E structure, K93 N−K91 O, I57 N−left-hand water (Figure 5B), K93 O−S56 OG, T94 OG1−E95 N, and E95 O−A97 N. Moreover, the carboxyl group of E95 is within 3.4 Å of the ϵ-amino group of K54, consistent with the formation of a salt bridge. Significant differences in the position of the peptide backbone in the region 94−97 for wild-type and G95E are shown in Figure 5C, where the backbone atoms, heme, and bound waters are overlaid. For example, the distance between the carbonyl oxygens of wild-type and G95E cytochrome c_2 are 0.12, 0.50, 0.85, 0.15, 0.42, and 0.26 Å for positions 93−98, respectively. The basic movement of the carbonyl oxygens at positions 95 and 97 is away from the heme. Moreover, each of the bound waters moves just over 0.3 Å, apparently to compensate for the shifts in the backbone and other minor adjustments. Thus, there are no dramatic structural changes in G95E relative to wild-type, but there are a number of small structural adjustments. A possible steric clash between the β-carbon of the glutamic acid at position 95 and adjacent heme atoms does not appear to be responsible for the structural changes observed, with the principal new interactions being five hydrogen bonds and a likely salt linkage between the E95 carboxyl and the ϵ-amino group of K54.

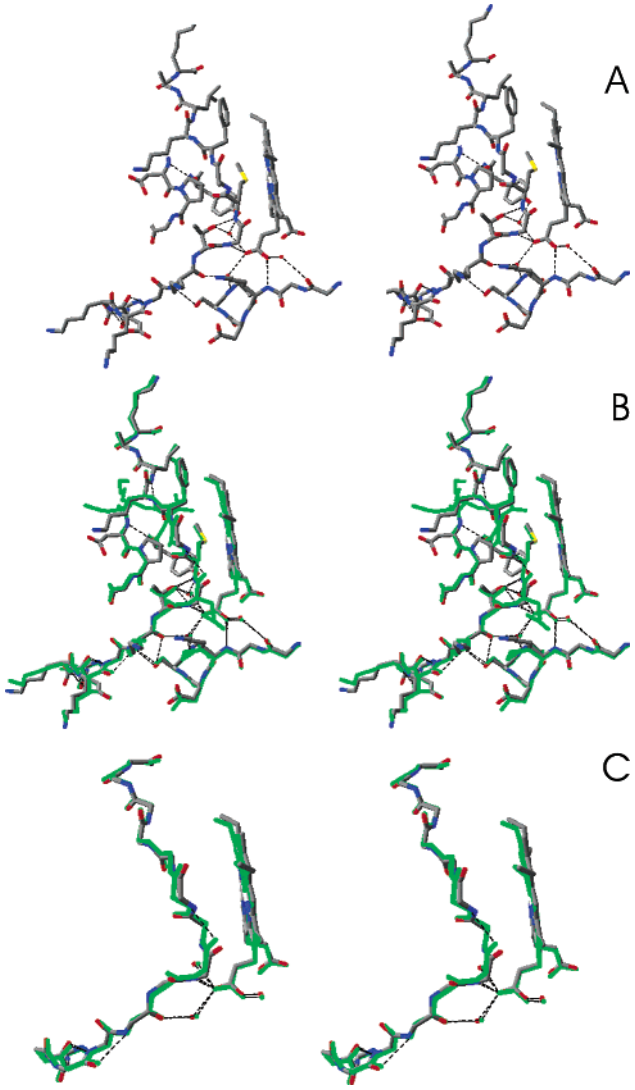

FIGURE 5: (A) Stereoview of the *Rb. capsulatus* cytochrome c_2 hinge (89−102) and adjacent regions (75−80, 52−57). Hydrogen bonds, as identified by Deep View, are dashed black lines. Shown are the backbone atoms, side chains, heme, and bound waters. For clarity, side chains at positions 52, 53, 57, 76, and 77 were omitted. (B) Superposition of wild-type (CPK) and G95E (green) in the hinge and adjacent regions. Shown are backbone atoms, side chains, heme, and bound waters. (C) Superposition of wild-type (CPK) and G95E (green) main chain atoms, hemes and bound waters.

DISCUSSION

Taking advantage of the kinetics and spectral properties of G95P, we were able to determine K_2 (1×10^6 M^{-1}) for this mutation. As discussed earlier, we computed k_{23}, k_{21}, and K_1, assuming the G95P K_2 value is a reasonable estimate for the hinge mutants and wild-type. Thus, all relevant parameters, kinetic and equilibrium have been *estimated* for wild-type and mutant *Rb. capsulatus* cytochromes c_2 (Table

1). Note that our underlying assumption is that the hinge mutants will not affect the heme electronic properties and will have only marginal effects on direct ligand binding (k_{23} in particular, because the hinge has presumably swung away from the heme face for ligand binding). This assumption does not necessarily hold for all mutants, particularly if the mutation alters the interaction of the protein chain with the bound imidazole. However, in this case, a significant effect on k_{32} would be likely. The four mutant groups, based on imidazole binding properties and presented in Table 1, will be discussed in turn.

Group 1 Mutants. The first group, including wild-type and the mutants K90E, K91E, K93E, A101G, and K102E, involves mutations that are relatively radical, with either a change in charge, in the size of the side chain, or in conformational flexibility of the backbone. Despite this diversity, all these cytochromes c_2 have basically similar imidazole binding properties (kinetic and equilibrium). Interestingly, all proteins in this first group have very similar properties in terms of resistance to denaturation, and their alkaline pK_a for the 695 nm transition (Table 2). Thus, it is reasonable to conclude that these substitutions do not have a significant effect on hinge dynamics. In these examples, the cytochrome is predominantly in the closed state (cyt, eq 1), on the order of 99.8−99.9% (based on K_1).

Group 2 Mutants. In contrast to the mutants discussed above, the second group (M96N) is in the open or high-spin state (cyt* in eq 1) and has an affinity ($\sim 6 \times 10^5$ M^{-1}) approaching that estimated for K_2 (1×10^6 M^{-1}) in wild-type and the mutants. Presumably, in this case, there is little or no closed form (cyt in eq 1); hence, a rate-limiting conversion to the open form is not observed. Interestingly, in terms of the concentration of guanidine-HCl required for denaturation (Table 2), it appears that M96N is substantially more stable than wild-type; however, the *m*-value is decreased significantly. Thus, the overall stability of M96N is similar to that for the wild-type cytochrome. Further analysis of the M96N mutant will have to await the determination of its structure.

Group 3 Mutants. The third group, consisting of K93P, VK93G, G95E, G95K, and G95P, has substantially altered imidazole binding and kinetics. Relative to wild-type, mutations at positions 93 (with the exception of K93E) and 95 have a number of common properties, including elevated values of K_{app} (7−31-fold), increased values of k_{12} (2−24-fold) and decreased values of k_{21} (1.2−10-fold). Note however, that k_{32} for the group 3 mutants is within a factor of 3 of that for wild-type. Clearly, positions 93 and 95 can influence the hinge kinetics and make the heme more accessible to imidazole. This general observation is consistent with detectable amounts of high-spin heme in the mutants at positions 93 and 95. As shown in Figure 5, the G95E mutation results in a number of small structural changes, which, based on the kinetics of imidazole binding, result in increased flexibility of the hinge (or part thereof). An obvious explanation for the effect of mutations at G95 is that they result in a loss of conformational flexibility, because glycine is the only amino acid without a side chain and the only one that can adopt conformations outside the allowed regions of the Ramachandran plot. However, both wild-type cytochrome c_2 and G95E adopt normal phi/psi angles within the allowed regions. Thus, the unique conformational flexibility of glycine cannot be the reason that mutations have such large effects at this position. A second possibility is that there is a steric clash in the mutants which is not present in the wild-type G95, which is adjacent to the heme. When we modeled the wild-type protein with an alanine at position 95, the distance of the beta carbon to the fixed carbons of the heme indicated that there is no steric clash (4.4 Å to the heme CAD and CMD carbons). The distance from the modeled beta carbon to the nearest atom, the front heme propionate O1D oxygen, was found to be 3.0 Å. However, in the crystal structure of mutant G95E, the beta carbon of the glutamic acid is 3.9 Å from the same heme propionate oxygen. Thus, a potential steric clash resulting in the twisting of the peptide backbone in the hinge region (positions 93−97) in G95E may drive structural changes that stabilize the hinge per se (5 additional hydrogen bonds, Figure 5B) but which weaken the interactions of the hinge with the heme, resulting in an increase in k_{12}. Note that, in principle, the front heme propionate could rotate to adjust for a steric clash. However, this could disrupt the extensive hydrogen bonding network involving the bound waters. The proximity of the G95E carboxyl to the K54 ϵ-amino group would further stabilize the mutant conformation. In both the G95P and the G95K mutants, steric repulsion with the propionate carboxyl would also lead to a weakening of the heme−hinge interaction by the same logic used in the G95E case, but with kinetic effects somewhat different for the three mutations at position 95 (Table 1) because of the different side chain properties (size, charge, etc.).

Rb. sphaeroides cytochrome c_2 and horse cytochrome c have naturally occurring variants at position G95 (K99 and K79, respectively), which suggests that they would show significantly different imidazole binding and kinetics for rearrangement based on the *Rb. capsulatus* cytochrome c_2 results described here. Nevertheless, it has been shown that these cytochromes are similar to the wild type *Rb. capsulatus* protein in terms of the value of k_{12} and, in the case of *Rb. sphaeroides* cytochrome c_2, of K_{app} as well. In fact, the alpha carbon of *Rb. sphaeroides* M100 (position 96 in *Rb. capsulatus*) has shifted about 0.5 Å away from the heme relative to *Rb. capsulatus* cytochrome c_2 (see Figure 1C), and the lysine side chain does not clash with other regions of the cytochrome. Furthermore, the structural equivalent of position K54 in *Rb. capsulatus* cytochrome c_2 is G58 in *Rb. sphaeroides*. Thus, it appears that the small changes in position (backbone, side chains, and bound waters), between *Rb. capsulatus* and *Rb. sphaeroides* cytochrome c_2, compensate for the amino acid difference at position 95/99, and do not affect the kinetics of imidazole binding.

In the case of K93, the lysine side chain extends into the solvent (Figure 5A) and does not form a salt bridge with any other amino acid side chain. Thus, substitution of the lysine with a glutamic acid has no measurable effect on the hinge kinetics. In contrast, the substitution with proline or glycine has a very substantial impact on K_{app} and k_{12}. As a consequence, these mutations affect K_1, consistent with a significant weakening of the interaction of the hinge with the rest of the protein. Presumably, a change in conformational flexibility with proline or glycine at this position permits a repositioning of the backbone and side chains in this region, resulting in altered kinetics. Structures of the K93P and VK93G mutants are needed to fully analyze the

structural changes induced by these mutations. The fact that substitution with both proline and glycine, which have very different side chain properties, affects K_1 suggests that a specific conformation in the region of position 93 is important for the stability and hinge movement and that both the glycine and proline mutants adopt conformations that prevent native folding.

Group 4 Mutants. The fourth group of mutants includes F98S and K99E. Mutant F98S is of particular interest because there is an extensive literature on the equivalent mutation in yeast (F82) (*12*−*17*), and it forms a close interaction with the heme. That is, it would appear from the structure to lock the hinge in place and reduce mobility. However, we found that mutant F98S has a nearly normal apparent binding constant (K_{app}) and rate constant for rearrangement (k_{12}), but k_{23}/k_{21} is 36-fold larger than that for wild type, and in fact, it is larger than that for any of the other mutants. Furthermore, k_{32} is 0.8 s^{-1} for F98S, which is larger than that for any other mutant and 14-fold larger than for wild-type, and k_{21} is decreased almost 3-fold (assuming that K_2 is the same for wild-type and F98S). The K99E mutation affects the kinetic and binding constants in a similar way, but with a smaller effect; k_{23}/k_{21} is 7-fold larger, and k_{32} approximately 4-fold larger, than that for wild-type. The lack of detectable high-spin heme and the large increase in k_{32} in F98S and K99E suggests that our assumption that K_2 is the same for wild-type and the hinge mutants may not be valid with these mutants. On the basis of the increase in k_{32}, it would appear that, in the imidazole−mutant complexes (F98S and K99E), the bound imidazole is more solvent accessible (or less sterically constrained) and thus more likely to dissociate. Using the *Rhodobacter sphaeroides* cytochrome c_2 − imidazole complex structure (Figure 1B), it appears that replacement of the phenylalanine with serine removes the hydrophobic interaction with the heme that may allow increased solvent and ligand access in the open form (cyt* in eq 1). The structure of the yeast cytochrome c F82S mutant shows that there are rearrangements of nearby side chains, but the main effect is to open a solvent channel to the heme (*12*). Thus, the imidazole binding constant (K_2) is strongly affected because of a markedly different environment in proximity to the bound ligand, distinct from that found with the mutations at positions 93 and 95. A similar, but smaller effect may be operative with K99E. K99 normally salt-bridges D78, but the mutation to glutamic acid at position 99 would break this salt-link and result in electrostatic repulsion. This may cause a repositioning of the side chain and backbone, increasing solvent access to the bound imidazole, effectively raising its pK_a, and thereby weakening the interaction with the heme iron. An alternative is that increased solvent access could alter the interaction of the bound imidazole with the surrounding protein matrix.

SUMMARY

Clearly, the mutations near the N− or C− terminus of the hinge peptide (88−102) have little effect on the hinge dynamics. This is consistent with the structural data that are available for *Rb. sphaeroides* cytochrome c_2, where the principal structural differences between wild-type and the imidazole complex are in the region 97−104 (93−100 in *Rb. capsulatus* cytochrome c_2), as shown in Figure 1A. Thus, from a dynamic point of view, the hinge appears to be constrained to positions 93−100. Within the 93−100 region, we have characterized mutations at positions 93, 95, 96, 98 and 99. Position 96 supplies the sixth heme ligand, and M96N changes the structure substantially but does not provide information relative to the hinge dynamics. Mutations at positions 93 and 95 have a profound effect on the hinge dynamics, apparently a consequence of altering the interactions with adjacent groups, leading to a destabilization of the heme−hinge interaction. Note that, based on the G95E structure, only small structural changes occur, but these, coupled with a new salt bridge between the G95E carboxyl and the K54 epsilon amino group, result in a twisting (relative to wild-type) of the backbone in G95E, which alters the heme−hinge interface. That is, these mutations alter the structure of the closed native form of cytochrome c_2, facilitating the conversion to the open form. In contrast, the mutations at positions 98 and 99 have little effect on the hinge dynamics but rather affect the imidazole binding constant through increased solvent access. To a first approximation, these mutations alter the structure of the open form of native cytochrome c_2.

REFERENCES

1. Schejter, A., and Aviram, I. (1969) The reaction of cytochrome c with imidazole, *Biochemistry 8*, 149−153.
2. Sutin, N., and Yandell, J. K. (1972) Mechanisms of the reactions of cytochrome c. Rate and equilibrium constants for ligand binding to horse heart ferricytochrome c, *J. Biol. Chem. 247*, 6932−6936.
3. Dumortier, C., Meyer, T. E., and Cusanovich, M. A. (1999) Protein dynamics: Imidazole binding to class I c-type cytochromes, *Arch. Biochem. Biophys. 371*, 142−148.
4. Dumortier, C., Holt, J. M., Meyer, T. E., and Cusanovich, M. A. (1998) Imidazole binding to *Rhodobacter capsulatus* cytochrome c_2. Effect of site-directed mutants on ligand binding, *J. Biol. Chem. 273*, 25647−25653.
5. Axelrod, H. L., Feher, G., Allen, J. P., Chirino, A. J., Day, M. W., Hsu, B. T., and Rees, D. C. (1994) Crystallization and X-ray structure determination of cytochrome c_2 from *Rhodobacter sphaeroides* in three crystal forms, *Acta Crystallogr. D50*, 596−602.
6. Berghuis, A. M., Guillemette, J. G., McLendon, G., Sherman, F., Smith, M., and Brayer, G. D. (1994) The role of a conserved internal water molecule and its associated hydrogen bond network in cytochrome c, *J. Mol. Biol. 236*, 786−799.
7. Banci, L., Bertini, I., Liu, G., Lu, J., Reddig, T., Tang, W., Wu, Y., Yao, Y., and Zhu, D. (2001) Effects of extrinsic imidazole ligation on the molecular and electronic structure of cytochrome c, *J. Biol. Inorg. Chem. 6*, 628−637.
8. Dumortier, C., Fitch, J., Meyer, T. E., and Cusanovich, M. A. (2002) Protein dynamics: Imidazole and 2-mercaptoethanol binding to the *Rhodobacter capsulatus* cytochrome c_2 mutant, glycine 95 proline, *Arch. Biochem. Biophys. 405*, 154−162.
9. Caffrey, M., Davidson, E., Cusanovich, M. A., and Daldal, F. (1992) Cytochrome c2 mutants of *Rhodobacter capsulatus*, *Arch. Biochem. Biophys. 292*, 419−426.
10. Benning, M. M., Wesenberg, G., Caffrey, M. S., Bartsch, R. G., Meyer, T. E., Cusanovich, M. A., Rayment, I., and Holden, H. M. (1991) Molecular structure of cytochrome c_2 isolated from *Rhodobacter capsulatus* determined at 2.5 A resolution, *J. Mol. Biol. 220*, 673−685.
11. Leys, D., Backers, K., Meyer, T. E., Hagen, W. R., Cusanovich, M. A., and Van Beeumen, J. J. (2000) Crystal structures of an oxygen-binding cytochrome c from *Rhodobacter sphaeroides*, *J. Biol. Chem. 275*, 16050−6.
12. Louie, G. V., and Brayer, G. D. (1989) A polypeptide chain refolding event occurs in the Gly82 variant of yeast iso-1 cytochrome c, *J. Mol. Biol. 209*, 313−322.
13. Louie, G. V., Pielak, G. J., Smith, M., and Brayer, G. D. (1988) Role of phenylalanine-82 in yeast iso-1-cytochrome c and remote conformational changes induced by a serine residue at this position, *Biochemistry 27*, 7870−7876.

14. Rafferty, S. P., Pearce, L. L., Barker, P. D., Guillemette, J. G., Kay, C. M., Smith, M., and Mauk, A. G. (1990) Electrochemical, kinetic, and circular dichroic consequences of mutations at position 82 of yeast iso-1 cytochrome c, *Biochemistry 29*, 9365−9369.
15. Concar, D. W., Whitford, D., Pielak, G. J., and Williams, R. J. P. (1991) The role of phenylalanine-82 in electron exchange reactions of eukaryotic cytochromes c, *J. Am. Chem. Soc. 113*, 2401−2406.
16. Lo, T. P., Guillemette, J. G., Louie, G. V., Smith, M., and Brayer G. D. (1995) Structural studies of the roles of residues 82 and 85 at the interactive face of cytochrome c, *Biochemistry 34*, 163−171.
17. Feinberg B. A., Liu, X., Ryan, M. D., Schejter, A., Zhang, C., and Margoliash, E. (1998) Direct voltammetric observation of redox driven changes in axial coordination and intramolecular rearrangement of the phenylalanine-82 histidine variant of yeast iso-1 cytochrome c, *Biochemistry 37*, 13091−13101.

BI0362370